International Journal of Earth, Energy and Environmental Sciences
ISSN: 2517-942X
Vol:5, No:3, 2011

Finite Element Modelling of Ground Vibrations Due to Tunnelling Activities

Muhammad E. Rahman and Trevor Orr

***Abstract*—**This paper presents the use of three-dimensional finite elements coupled with infinite elements to investigate the ground vibrations at the surface in terms of the peak particle velocity (PPV) due to construction of the first bore of the Dublin Port Tunnel. This situation is analysed using a commercially available general-purpose finite element package ABAQUS. A series of parametric studies is carried out to examine the sensitivity of the predicted vibrations to variations in the various input parameters required by finite element method, including the stiffness and the damping of ground. The results of this study show that stiffness has a more significant effect on the PPV rather than the damping of the ground.

***Keywords*—**Finite Elements, PPV, Tunnelling, Vibration

I. Introduction

THE environmental effects of noise and vibrations have received considerable attention in recent years due to the damage that vibrations can cause to buildings and because of the sensitivity of people to noise and vibration [1, 2]. Vibrations can be generated either by natural or artificial sources. Natural sources are earthquakes, ocean waves and landslide. In the case of earthquakes, the intensity of ground vibrations may be high enough to result in severe structural damage or even collapse of structures accompanied by loss of life [3]. Ground vibrations from artificial sources are called man-made vibration. Sources of man-made vibrations include machinery, compressors, pile drivers, road traffic, tunnel construction, mechanised construction activities, demolition of structures and aircraft. The magnitude of man-made vibrations is normally much smaller compared to earthquake vibrations and hence these vibrations do not, in most cases, cause serious structural damage to buildings and their effects are limited to the development of cosmetic cracks in the walls and floors. Man-made vibrations can also induce densification in sandy soils, resulting in foundation settlement. This settlement has the potential of inducing more serious structural damage than the cosmetic cracking that results from direct vibration due to machinery in the building itself [3].

Muhammad E. Rahman is with the Curtin University Sarawak, Miri, Sarawak, Malaysia (corresponding author phone: 60-128451750; e-mail: merahman@curtin.edu.my).

Trevor Orr is with the University of Dublin, Trinity College, Dublin-2, Ireland.

Tunnelling under city streets has now become a common activity for nearly all the types of transportation, but long urban tunnels are principally for metros, water supply and sewers. Shorter tunnels may be required for highway underpasses and pedestrian subways. Longer highway tunnels are sometimes suggested but problems of access and ventilation add greatly to their difficulty and cost, against which preservation of surface land and gains in environmental amenity may prove a quite inadequate offset [4, 5]. It is necessary to ensure that structures of historic and economic importance will not be affected or that any effects will be within acceptable limits. Vibration from tunnelling activities will normally be of a temporary nature and much smaller than earthquake vibrations[6, 7, 8, 9, 10].

The consequences of tunnelling activities have prompted recent research into improved methods for predicting the ground vibrations induced by tunnelling in free field conditions and in houses. This paper presents the use of three-dimensional finite elements coupled with infinite elements to predict the ground vibrations at the surface level in terms of the PPV due to construction of the Dublin Port Tunnel.

II. Dublin Port Tunnel

The Dublin Port Tunnel project comprises approximately 5.6km of dual carriageway, of which 4.5km are underground, with 2.1km of twin cut and cover tunnels and 2.4km of twin-bored tunnels, plus associated interchanges and infrastructure. It provides a link from Dublin Port to Santry in the Dublin suburbs and the motorways to the rest of Ireland. The depth of the bored tunnel section, from existing ground level to the roof of the tunnel, ranges from approximately 19m to 24m under residential houses.

III. Ground Conditions

The ground conditions within the tunnel area consist of glacial deposits resting on limestone bedrock. In many areas along the route of the tunnel these deposits are overlaid by made ground of varying thickness, which is site specific. Rock head levels along the line of the tunnel are relatively close to the surface and generally vary from 5 to 20m below the ground level. Due to the irregular profile of the rock head, the ground cover can change significantly over a short distance. The water table is at around 1m below the ground level.

The glacial deposits consist of brown boulder clay underlain by black boulder clay. The brown boulder clay consists of stiff sandy silty clay and sandy clayey silt with some gravel. The black boulder clay can generally be described as very stiff to hard slightly sandy clay with much fine to coarse, subrounded to subangular, limestone gravel and occasional cobbles and boulders. The underlying Dublin formation bedrock comprises carboniferous limestone and shales known as 'Calp' limestone. The limestone can be described as a predominantly strong to very strong, very thin to medium bedded, dark grey, predominantly medium to coarsely crystalline and fossiliferous limestone, with occasional interbedded, moderately strong, very thin to thin, dark grey to black, unweathered shaley mudstones and strong to very strong fine grained argillaceous limestone [11]. The limestone within the project area lies wholly beneath the water table with artesian pressure to near surface observed in piezometers. Water inflows during tunnelling in the limestone were generally around 250litres/min for the full 11.8m diameter. The ground conditions were modelled as three different layers of soil strata and the values of the material properties used for the each layer were based on the results of ground investigations. The material properties that were used in the finite element analyses are given in Table I.

TABLE I
VALUES OF SOIL PARAMETERS USED IN REFERENCE MODELS

	Top layer	DBC[1]	Limestone	Concrete	Steel
Density, kN/m^3	20	23	27	24	78
Young's modulus, GPa	0.2	1.0	60	40	200
Poisson's ratio	0.49	0.49	0.25	0.2	0.3
Damping, %	2.85	1.75	1.0	1.0	0.5

[1]DBC= Dublin Boulder Clay

IV. EMPIRICAL MODELS

As so many variables are involved in the determination of vibration levels in the ground due to tunnelling, no explicit equations exist which allow the magnitude of the ground vibrations at the surface to be predicted accurately for any given source and ground conditions. Approximate empirical equations have been developed based on a limited number of case studies, and these concentrate on the simulated resultant peak particle velocity at the ground surface. Prediction methods are required that can predict the ground vibrations taking account of both the nature of the activity causing the vibrations and the characteristics of site. Mechanised tunnelling generates levels of groundborne vibration that are unlikely to cause damage to structures.

Godio et al., (1992 cited in Hillar & Crabb, 2000) proposed an equation for predicting an upper bound to the peak particle velocities, v in mm/s due to ground vibrations. This is a useful first estimate for the vibration levels likely to be generated by mechanised bored tunnelling works and is given by the Equation (1):

$$v = Ar^{-1.3} \quad (1)$$

where A is a constant whose value depends on the ground condition (for hard ground A=180) and r is the direct distance (m) from the vibration source to the measurement location.

Nishimatsu also produced equations for upper and lower bounds for v based on monitored vibration values on other construction sites. Their upper and lower bound equations for the peak particle velocity are:

$$v = 176r^{-1.18} \quad \text{(upper bound)} \quad (2)$$

$$v = 7.4r^{-1.07} \quad \text{(lower bound)} \quad (3)$$

V. NUMERICAL MODELLING

Three dimensional finite element models were used in this paper to predict the ground vibrations at the surface. Three-dimensional finite element models allow the analyst to account for the extent and geometry of each of stratum when constructing a representative numerical model to predict the ground vibrations due to the TBM. The problem to be analysed is shown in Fig. 1. In Fig. 1, the geometry is idealised by a finite region (Part I) and a semi-infinite far field region (Part II). The ABAQUS V6.4 finite element software was used to construct the model and three-dimensional eight noded linear brick and reduced integration elements, C3D8R, were employed for the ground and the tunnel lining which is under Part I. Reduced-integration elements use fewer integration points in each direction than the fully integrated elements. These reduce the running time, especially in three-dimensional finite element analyses. In Part II, the soils and tunnel lining in the far field that extends to infinity, were modelled by the infinite elements, CIN3D8. In the model, the top layer is brown clay, the middle layer is Dublin boulder clay and the bottom layer is limestone. The finite element mesh is shown in Fig. 2. The elementary boundary conditions are applied on the four sides of the vertical section to obtain horizontal fixities, which allow only vertical movement, and these boundaries are also applied on the bottom side to obtain a full fixity [12].

The dimensions of the finite element model are 132m in the transverse direction, 50m in the vertical direction and 40m in the direction of the tunnel. The thickness of the top layer is 2.5m, the middle layer is 11m and the bottom layer is 36.5m.

By advancing in the ground, the tunnel-boring machine is a vibrating source from which vibrations are transmitted into the ground. Therefore, the impacts of the TBM on the ground during boring have been modelled by a dynamic loading system. The finite elements representing the TBM cutter have been loaded by a short triangular pulse. Due to this pulse, waves propagate through the soil and the response at the surface is determined. The analyses have been carried out in the time domain.

VI. NUMERICAL RESULTS

Finite element models were constructed of the ground, the tunnel lining and the frame of the TBM at different sections along the tunnel bore. Consistent modelling techniques were used for each section points with material properties for the ground of these sections based on ground investigations.

The choice of element to be used for the ground, the tunnel lining and the frame of the TBM is limited in ABAQUS V6.4 because the three-dimensional eight noded linear brick and reduced integration element, C3D8R, is the only element available both in the continuum solid element and the infinite element family. Eight-noded linear brick elements with a linear material model have been used to define the ground, the tunnel lining and the frame of the TBM.

In each case, the thicknesses of the different layers of ground were selected from the ground investigation information and extended in the tunnel direction to generate the solid model. For simplification, the material properties in each layer were assumed to be constant in the tunnel direction and in the transverse direction in the three-dimensional finite element model.

VII. RESULTS AND DISCUSSION

The vibrations were generated in the finite element model by applying a unit triangular pulse (Fig. 3) to the ground in front of frame of the TBM. The output results presented in Fig. 4 and Fig. 5 are the ground response in the transverse direction on the surface just above the TBM in the time domain and the frequency domain respectively at measuring Section 1 due to the unit triangular pulse. In Fig. 4, it can be seen that the finite element predicted ground vibrations are free from any reflections and this indicates that the infinite elements in ABAQUS are working effectively. In Fig. 5 it can be seen that the frequency band of greatest vibration amplitudes is in the range of 8 to 30Hz and peak amplitudes occurs at 18Hz. Fig. 6 shows the measured TBM excitation in the transverse direction at measuring Section 1 in the time domain and Fig. 7 is the Fast Fourier Transform (FFT) of Fig. 6 and shows that most of the energy is concentrated in the frequency range of 3 to 30Hz; these are also called the source function. Fig. 8 shows the vibration velocity v(ω) in the transverse direction plotted against frequency, which derived from the following equation:

$$v(\omega) = F(\omega)*\{\text{output}(\omega)/\text{input}(\omega)\} \quad (4)$$

where $F(\omega)$ is the source function, i.e. the TBM excitation.

Fig. 9, Fig. 10 and Fig. 11 show the vibration velocity at the surface level just above TBM at measuring Section 1 in the time domain in the three orthogonal directions (x, y and z) due to the transverse input load. The peak particle velocity due to a transverse load and the resultant peak particle velocity are calculated using Equations 5 and 6 respectively [14].

Peak Particle Velocity (PPV) due to a transverse load

$$(T_{PPV}) = \sqrt{T_x^2 + T_y^2 + T_z^2} \quad (5)$$

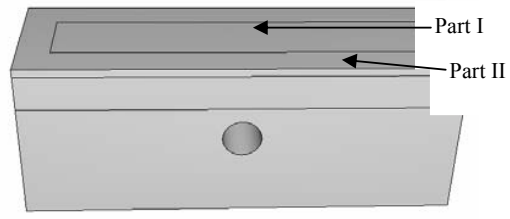

Fig. 1 Typical model

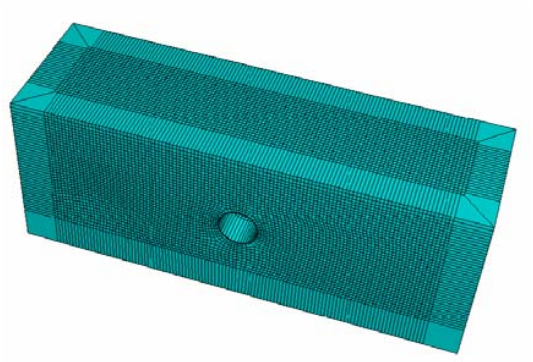

Fig. 2 Finite element mesh

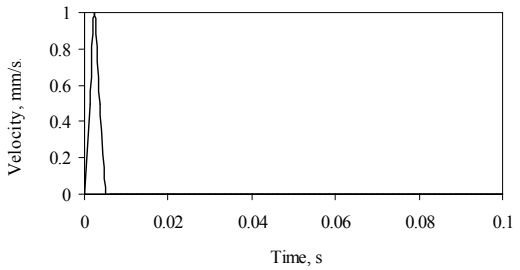

Fig. 3 A short triangular pulse

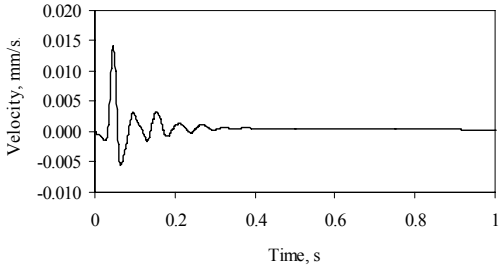

Fig. 4 Predicted time history in surface level at measuring Section 1; transverse direction

$$\text{Resultant PPV} = \sqrt{T_{PPV}^2 + V_{PPV}^2 + L_{PPV}^2} \quad (6)$$

where T_x = Vibration velocity in x direction (transverse) due to a transverse input load

T_y = Vibration velocity in y direction (vertical) due to a transverse input load

T_z = Vibration velocity in z direction (longitudinal) due to a transverse input load

T_{PPV} = Peak Particle Velocity (PPV) due to a transverse input load
V_{PPV} = Peak Particle Velocity (PPV) due to a vertical input load
L_{PPV} = Peak Particle Velocity (PPV) due to a longitudinal input load.

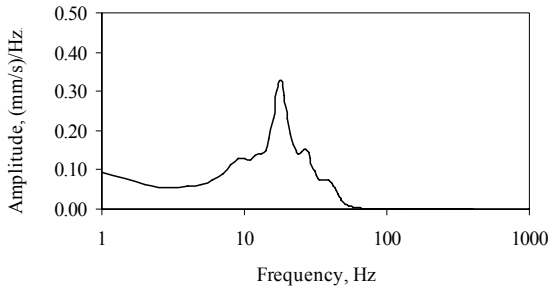

Fig. 5 FFT of time history in surface level at measuring Section 1; transverse direction

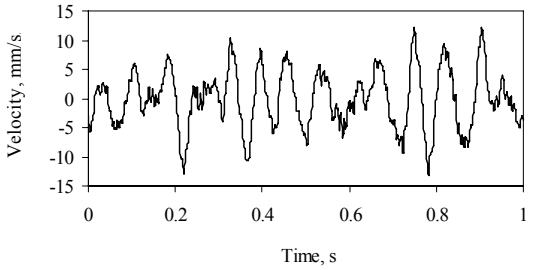

Fig. 6 Measured TBM excitation at measuring Section 1; transverse direction

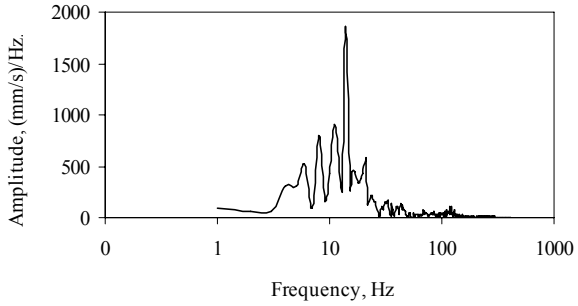

Fig. 7 FFT of TBM excitation at measuring Section 1; transverse direction

The 3-D FE predicted resultant PPV values together with the Godio and Nishimatsu upper and lower bound values are plotted in Fig. 12, 13, 14 and 15. The PPV values plotted in Fig. 12, 13, 14 and 15 show that there is good agreement between the 3D-FE predicted values and the Godio and Nishimatsu upper and lower bound values. It can be seen from the results plotted for each section that the 3D-FE lie between the Godio and Nishimatsu upper and lower bound values. It can also be seen from Fig. 12, 13, 14 and 15 that all the models have similar attenuation characteristics. Empirical models are a function of only the direct distance between

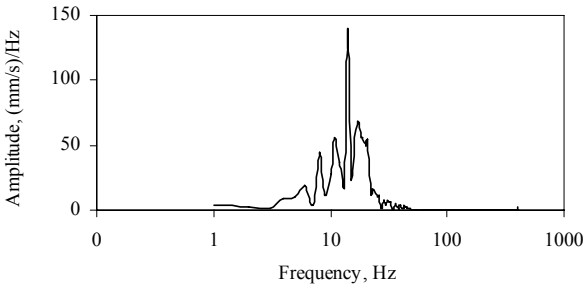

Fig. 8 Transverse vibration velocity (Frequency domain) at the surface at measuring Section 1; transverse direction

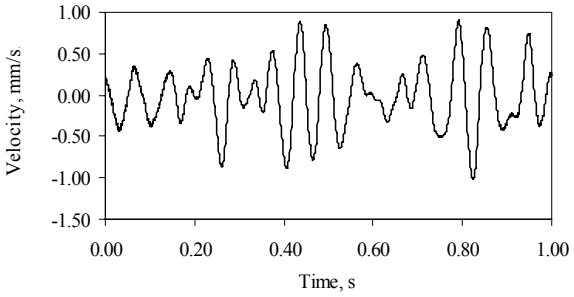

Fig. 9 Transverse vibration velocity at the surface level measuring Section 1 due to transverse vibration.

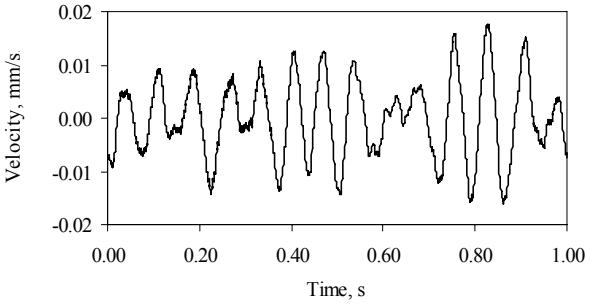

Fig. 10 Vertical vibration velocity at the surface level at measuring Section 1 due to transverse vibration

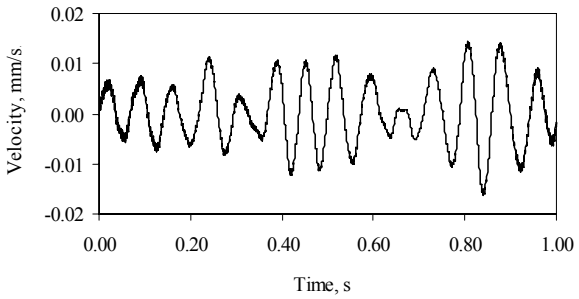

Fig. 11 Longitudinal vibration velocity at the surface level at measuring Section 1 due to transverse vibration

the source and the point of interest, while the groundborne vibrations depend also on the soil properties particularly, on the stiffness and the resonance frequency of the soil layer, and on the tunnel boring machine excitation.

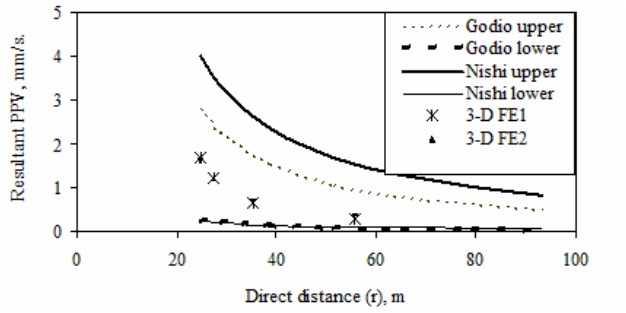

Fig. 12 FE, empirical and measured PPV values at Section 1

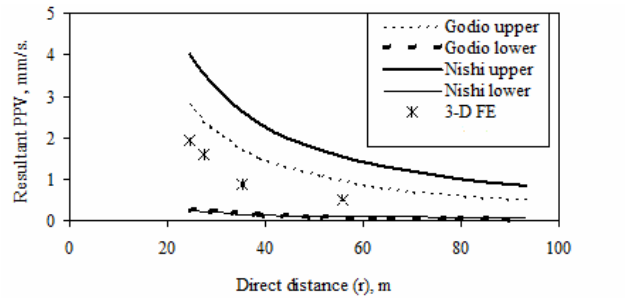

Fig. 13 3D-FE, empirical and measured PPV values at Section 2

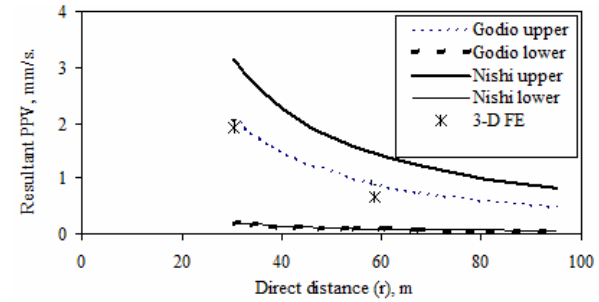

Fig. 14 3D-FE, empirical and measured PPV values at Section 3

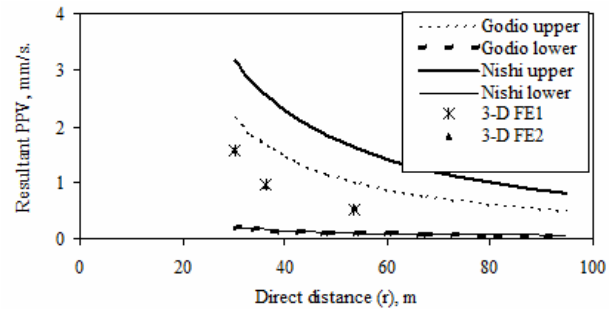

Fig. 15 3D-FE, empirical and measured PPV values at Section 4

VIII. Parametric Study

The level of vibration observed at any point depends on the energy transmitted into the ground at the source and its subsequent attenuation within the ground. In this section, the results of a series of parametric studies to examine the sensitivity of the vibration predictions to variations in the various input parameters, which include the stiffness and the damping properties of the soil, are discussed.

TABLE II
RANGES OF PARAMETERS USED IN SENSITIVITY ANALYSES

	Top layer	DBC[1]	Limestone	Concrete	Steel
Stiffness, GPa	0.01, 0.1, 0.2, 0.5, 1.0	1.0	60	40	200
Frequencies Ranges, Hz	8 to 35 1 to 60	8 to 35 1 to 60	8 to 35 1 to 60	8 to 35 1 to 60	8 to 35 1 to 60
Damping, %	2.85	1.75	1.0	1.0	0.5

[1]DBC= Dublin Boulder Clay

TABLE III
NORMALISED PPV WITH RESPECT TO REFERENCE MODEL

Frequency Range	-10m from TBM face	At TBM face	+10m from TBM face
8 to 35 Hz (Reference)	1.0	1.0	1.0
1 to 60 Hz	1.1	1.18	1.05

The Nishimatsu supplied the values of the material parameters used for the finite element modelling of the strata. The samples of soil were collected at different locations and different depths along the tunnel line for testing in the laboratory. Field tests were also carried out to determine the values of the soil parameters required for the design of the tunnel and for use in the finite element analyses.

A. The Effects of Varying the Stiffness of the Soil

A reference model of the ground was selected in which the soil parameter values were based on the results of the soil tests. The parameters required for the dynamic analyses were the weight density, dynamic Young's modulus, Poisson's ratio and the damping ratio and the values of these parameters are given in Table I.

In order to investigate the effect of variations in the material parameters on the produced vibrations, the stiffness of the upper soil layer of the reference model was changed. The range of values used in this study for the soil parameters in the upper soil layer are summarised in Table II.The results of the parametric study on the effects of the upper layer's modulus of elasticity on the amplitude of the vibrations are presented in Fig. 16, 17 and 18. As can be seen in Fig. 16, the resonance frequency increases with increasing the stiffness of the upper soil layer. The resonance frequency is dependent on the stiffness of the soil layer. When the resonance frequency of the soil layer and the TBM excitation coincide or are very close, this results in a maximum vibration velocity. In Fig.16, it can be seen that the resonance frequency of the soil layer at upper layer's stiffnesses of 0.01GPa, 0.1GPa, 0.2GPa, 0.5GPa and 1.0GPa are 4Hz, 15Hz, 18Hz, 20Hz and 22Hz respectively and in Fig. 7 the resonance frequency of the TBM

excitation is 14Hz. Since the resonance frequency of 15Hz of the soil layers at stiffness 0.1GPa of upper soil layer is very close to the resonance frequency of 14Hz of the TBM excitation, the maximum vibration velocity is obtained at this stiffness which is shown in Fig. 17. The minimum vibration velocity is obtained at stiffnesses of upper soil layer of 0.01 GPa and 1.0 GPA, since at these stiffnesses there is a significant difference between the resonance frequency of the soil layer and the resonance frequency of the TBM excitation. Fig. 18 shows the variations of velocity reduction with the distance. The vibrations at points on the ground surface directly above the tunnel axis and up to 50m an either side are most sensitive to variations in the stiffness of the upper soil layer. After 50m from the tunnel axis the influence of the material parameters on the surface vibrations is very small.

B. The Effects of Varying the Damping of the Soil

The damping ratio of the soil is a parameter that is difficult to determine. Often the damping ratio is chosen as 1-6% of the critical damping ratio. In the finite element code, the damping matrix, C is defined as a having two components, one proportional to the mass and the other proportional to the stiffness [15]:

$$[C] = \alpha [M] + \beta [K] \quad (7)$$

where [K] is the stiffness matrix, [M] is the mass matrix, [C] is the damping ratio matrix, α is the coefficient of mass damping and β is the coefficient of stiffness damping.

In this formulation of the damping, two frequencies can be chosen at which a given proportional damping applies. At other frequencies, the damping ratio will be different. Figure 19 shows two cases. In the reference model, the frequency is chosen so that it is exactly 1.0% at 8 and 35 Hz. In that case, the damping ratio is close to 1.0% between 8 and 35 Hz. However, at lower and larger frequencies, the damping ratio is considerably larger. The two frequencies values at which the damping ratio matches the given value should not be far away from each other. In Fig. 19 can be seen that the damping ratio will drop to 0.28% if the lower and upper bounds are 1 and 60 Hz; i.e. if the chosen frequency range is wide, the damping will be small between the lower and upper bound frequencies.

In order to investigate the effect of the material parameters on the results, the frequency range to calculate the α and β values for the reference model have been changed. The data used in this study are summarised in Table II.

Over the whole frequency range the response function will increase if the chosen frequency range is wide and consequently the amplitude of the vibrations will increase. It can be seen from Fig. 20 and Fig. 21 that the response function increased with increasing the chosen frequency range. The normalised results of the parametric study on the effects of the damping are presented in Table III. In Table III, it can be seen that the vibration velocity increases with increasing the frequency ranges i.e. with decreasing damping value. However, the increase in the vibration velocity is the highest on the surface directly above the TBM and decreases with distance from the tunnel face.

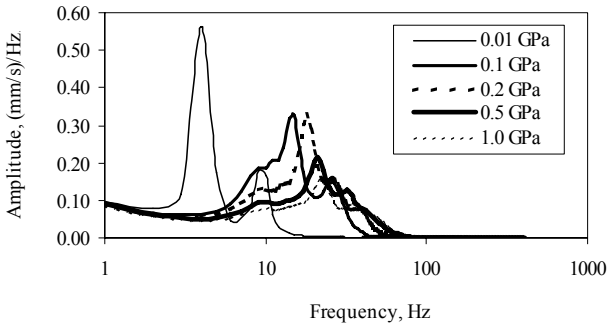

Fig. 16 Transverse output response (frequency domain) in surface level

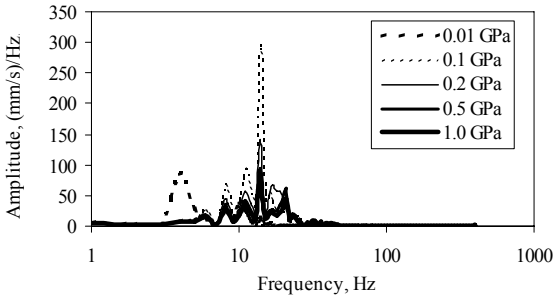

Fig. 17 Transverse vibration velocity (Frequency domain) in surface level

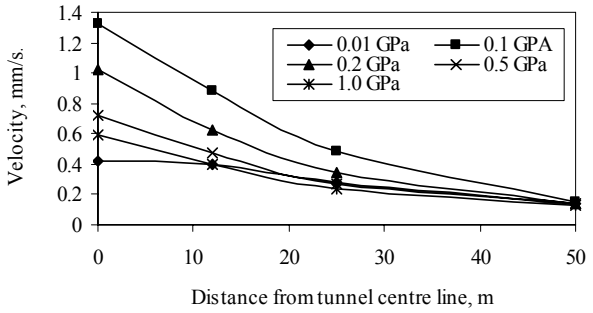

Fig. 18–The effects of stiffness on ground surface vibration

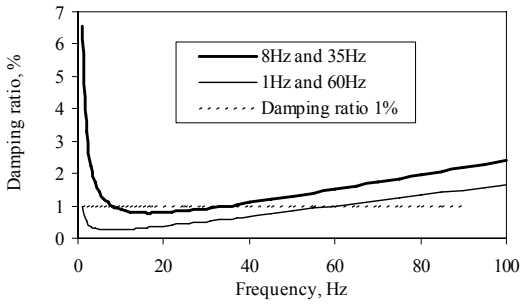

Fig. 19 Damping ratio of 0.01 (1%) dependent on frequency

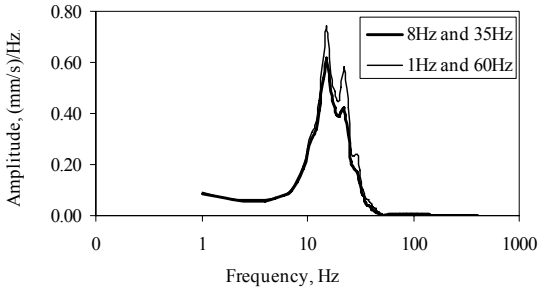

Fig. 20 Response function on surface directly above the TBM face

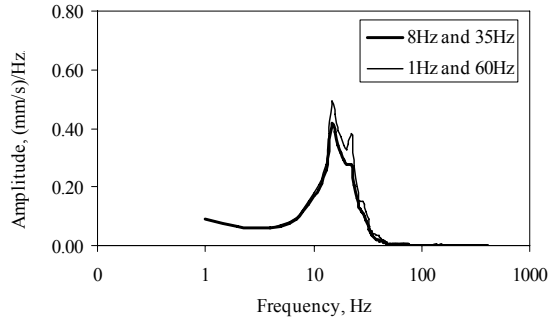

Fig. 21 Response function on surface at 10m behind of the TBM face

IX. Conclusion

3-D finite element analyses have been carried out to predict the TBM induced ground vibrations at the surface level. Although 3-dimensional finite element analyses are very time consuming, good agreement has been found, in terms of PPV, between the empirical model PPV values at the surface and the values calculated using 3-D finite element analyses. Based on the predictions, it is concluded that the surface vibrations are low enough not to cause any damage to structures on the surface. Empirical models are crude at best, as these are a function of only the direct distance between the source and the point of interest, while the groundborne vibrations also depend on the soil properties and especially on the stiffness and the resonance frequency of the soil layer, and on the tunnel boring machine excitation.

The stiffness of the ground is a most important parameter, which affects the resonance frequency of the ground. If the resonance frequency of the ground coincide with the resonance frequency of the TBM excitation or is very close to it, this will lead to larger vibrations level and vice versa. In the Dublin Port Tunnel, these two-resonance frequencies are quite close and yielded higher surface vibrations. Changes in the stiffness of the ground close to the tunnel have significant effects on the surface vibrations, while changes in the stiffness of the ground further away from the tunnel have less effect on the surface vibrations.

In the finite element, formulation the damping is defined as a combination of mass matrices and stiffness metrics. The differences between the results are small indicating that the effects of the damping ratio on the surface vibrations are insignificant compared to the effect of vibrations in the stiffness.

Acknowledgment

The work was carried out at the Department of Civil Engineering, University of Dublin, Trinity College. The project was supported by the Nishimatsu Construction Co., Ltd and the Geotechnical Trust Fund of the Institution of Engineers of Ireland. This support is gratefully acknowledged.

References

[1] Hillar, D.M., Hope, V.S., "Groundborne vibration generated by mechanised construction activities," Proceedings Institution of Civil Engineers: Geotechnical Engineering, vol. 131, no. 4, pp 223-232, 1998.
[2] Hall, L., "Simulations and analyses of train-induced ground vibrations in finite element models," Int. J. of Soil Dynamics and Earthquake Eng., vol. 23, pp 403-413, 2003.
[3] Athanasopoulos, G.A., Pelekis, P.C., "Ground vibrations from sheet pile driving in urban environment: measurements, analysis and effects on buildings and occupants," Int. J. of Soil Dynamics and Earthquake Eng., vol. 19, pp. 371-387, 2000.
[4] Megaw, T. M., Bartlett, J.V., "Tunnels-Planning, Design, Construction," Ellis Horwood Ltd Chichester, 1983.
[5] Burd, H.J., Houlsby, G.T., Augarde, C.E., Liu, G., "Modelling the effects on masonry buildings of tunnelling-induced settlement," Proceedings Institution of Civil Engineers: Geotechnical Engineering, vol. 143, pp. 17-29, 2000.
[6] Whyley, P.J., Sarsby, R.W., "Ground borne vibration from piling" Ground Engineering, vol. 26, pp. 32-37, 1992.
[7] New, B.M., "Ground vibration caused by construction works," Tunnelling and Underground Space Technology, vol. 5, pp. 179-190, 1990.
[8] New, B. M., "Vibration caused by underground construction. Tunnelling '82," The Institution of Mining and Metallurgy, pp. 217-229, 1982.
[9] Flanagan, R.F., "Ground vibration from TBMs and shields," Tunnels & Tunnelling, vol. 25, no. 10, pp 30-33, 1993.
[10] Kramer, S.L., "Geotechnical Earthquake Engineering," Prentice Hall, New Jersey, 1996.
[11] Farrell, E.R., O'Brien, S, Lehane, B., Orr, T., "Stiffness of Dublin Black Boulder Clay," Proceedings XI ECSMFE, Copenhagen, pp 1-6, 1995.
[12] Potts, D. M., Axelsson, K., Grande, L., Schweiger, H., Long. M., "Guidelines for the use of advanced numerical analysis," Thomas Telford London, 2002.
[13] Hillar, D. M., Crabb, G. I., "Groundborne vibration caused by mechanised construction works," Report TRL, No-429, pp1-79, 2000.
[14] Head, J.M., Jardine, F.M., "Ground-borne vibrations arising from piling," CIRIA Technical Note 142, 1992.
[15] ABAQUS, "Analysis User's Manual", Hibbit, Karlsson & Sorensen, ABAQUS Europe BV, Maastricht, The Netherlands, 2004.